

Photoionization of neutral atoms by X waves carrying orbital angular momentum

Robert A. Müller,^{1,2,3,*} Daniel Seipt,^{3,4} Randolph Beerwerth,^{3,4} Marco Ornigotti,⁵ Alexander Szameit,⁵ Stephan Fritzsche,^{3,4,6} and Andrey Surzhykov^{1,2}

¹Physikalisch-Technische Bundesanstalt, D-38116 Braunschweig, Germany

²Technische Universität Braunschweig, D-38106 Braunschweig, Germany

³Helmholtz-Institute Jena, D-07743 Jena, Germany

⁴Theoretisch-Physikalisches Institut, Friedrich-Schiller-Universität Jena, D-07743 Jena, Germany

⁵Institute of Applied Physics, Friedrich-Schiller-Universität Jena, D-07743 Jena, Germany

⁶Abbe Center of Photonics, Friedrich-Schiller-Universität Jena, D-07743 Jena, Germany

(Received 27 June 2016; published 21 October 2016)

In contrast to plane waves, twisted or vortex beams have a complex spatial structure. Both their intensity and energy flow vary within the wave front. Beyond that, polychromatic vortex beams, such as X waves, have a spatially dependent energy distribution. We propose a method to measure this (local) energy spectrum. The method is based on the measurement of the energy distribution of photoelectrons from alkali-metal atoms. On the basis of our fully relativistic calculations, we argue that even ensembles of atoms can be used to probe the local energy spectrum of short twisted pulses.

DOI: [10.1103/PhysRevA.94.041402](https://doi.org/10.1103/PhysRevA.94.041402)

In atomic physics, light is described by a plane wave in the majority of cases. In optics, however, methods are known to produce specially tailored *twisted* or *vortex* beams [1–5]. These beams have a helical, “corkscrew”-like, phase structure and can carry orbital angular momentum (OAM) in addition to their spin angular momentum [6–10]. Both the intensity and the energy flow of such beams depend on the position in the wave front [11,12]. Even though the interaction of twisted light and atomic targets has attracted much interest during recent years [13–16], only a few proposals have been made so far as to how one can study this internal structure of the beam itself [11,12,17]. In these proposals, however, only monochromatic beams were considered. Nowadays, much effort is spent to produce ultrashort twisted pulses, with the aim to benefit from OAM carrying light in the domain of optical pulses and spectroscopy [5]. In particular, recent experiments report the generation of twisted femtosecond pulses in the visible regime [18,19], Laguerre-Gauss supercontinua [20], and vortex light bullets [21,22]. Moreover, first signatures of OAM have been observed in XUV pulses from high harmonic sources [23–25] and free-electron lasers [26–28]. Obviously, such short pulses are not monochromatic but have a distribution of photon energies. Measured by detectors with spatial resolution, this energy distribution will depend on the position of detection in the beam. In analogy to the local energy flow, we will refer to this as the local spectrum of the twisted pulse.

Bessel beams are a special kind of twisted light. Pulses formed by such beams are also known as Bessel- X pulses [29] or X waves [30] and feature a localization in both space and time. For this reason, X waves have been the subject of intensive research in various fields, including optics [31–33], condensed matter [34], and waveguide arrays [35,36], to name just a few. In most of these works only zeroth-order Bessel- X pulses have been considered. Only recently have optical X

waves of higher order been introduced [37–39]. In these works it has been found that the orbital angular momentum has a pulse shortening effect on the X wave and causes a blueshift of the pulse’s carrier frequency.

X waves of nonzero order are expected to be of use in various areas of physics, such as material processing, spatially resolved spectroscopy, and optical communications. In all these cases, a characterization of the internal structure of such light fields will help to further optimize their properties for the desired applications. Up to now, however, only global characteristics such as time duration and carrier frequency of OAM-carrying X waves have been explored in some detail [37,38], whereas a complete characterization of their local spectrum has not been addressed yet. Here, we therefore propose an easy and reliable method for obtaining a full characterization of the local spectrum of X waves, based on the measurement of the photoelectron spectra of alkali-metal atoms. These atoms are widely used in experiments and can be very well described theoretically. Moreover, their ionization threshold is low enough to allow for single-photon ionization with available experimental techniques and, hence, the application of first-order perturbation theory. Therefore, alkali-metal atoms are particularly suited for studies aiming for a comparison between theory and experiment. Throughout this Rapid Communication, atomic units are used unless specified otherwise.

In order to construct a short twisted pulse, we start with a continuous Bessel beam that propagates along the z axis. Mathematically, such a Bessel beam can be expressed as a superposition of circularly polarized plane waves with frequency ω and helicity λ that all lay on a cone in momentum space [15,16],

$$\mathcal{A}_{xm\lambda}^{tw}(\mathbf{r}, t) = \int \frac{d^2\mathbf{k}_\perp}{(2\pi)^2} a_{xm}(\mathbf{k}_\perp) e^{i(\mathbf{k} \cdot \mathbf{r} - \omega t)} \mathbf{u}_\lambda, \quad (1)$$

where the momentum \mathbf{k} of each plane wave splits into a component $\mathbf{k}_\perp = (k_\perp, \phi_k, 0)$ perpendicular and a component $k_\parallel = (0, 0, k_z)$ parallel to the propagation axis. The cone

*robert.mueller@ptb.de

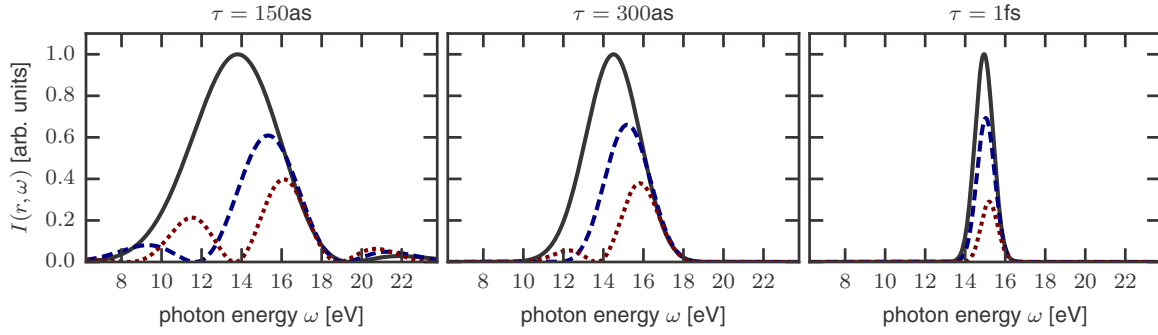


FIG. 1. Local spectrum $I(r, \omega)$ of an X wave of length $\tau = 150$ as (left panel), $\tau = 300$ as (center panel), and $\tau = 1$ fs (right panel). Results are shown for a pulse with $\omega_0 = 15$ eV, $\lambda = 1$, $m = 2$, $\theta_k = 10^\circ$ at three different distances from the beam axis ($r = 300$ nm: black solid line; $r = 500$ nm: blue dashed line; $r = 700$ nm: red dotted line). All results have been normalized to the maximum in each panel.

function

$$a_{\kappa m}(\mathbf{k}_\perp) = (-i)^m \sqrt{\frac{2\pi}{k_\perp}} e^{im\phi_k} \delta(k_\perp - \kappa), \quad (2)$$

determines the transversal momentum κ of the twisted beam and the total angular momentum (TAM) projection m upon the z axis. To conveniently compare beams with different ratios of transverse and longitudinal momentum, one often specifies the so-called *opening angle* $\theta_k = \arctan(\kappa/k_z)$ of the momentum cone instead of the transverse momentum κ .

To construct an X wave with duration τ , we convolute the vector potential (1) over a Gaussian spectral distribution while keeping the opening angle θ_k constant. For a pulse with spectral width $\Delta\omega = 1/\tau$ and central frequency ω_0 , the convoluted vector potential reads

$$A_{\theta_k m \lambda \omega_0}^{tw}(\mathbf{r}, t) = \int_0^\infty \frac{d\omega}{\sqrt{2\pi} \Delta\omega} e^{-\frac{1}{2}(\frac{\omega - \omega_0}{\Delta\omega})^2} \mathcal{A}_{\kappa m \lambda}^{tw}(\mathbf{r}, \omega). \quad (3)$$

From the Fourier transform $A_{\theta_k m \lambda \omega_0}^{tw}(\mathbf{r}, \omega)$ of this vector potential, we can obtain the intensity $I(r, \omega)$ of the beam. This intensity is a measure for the number of photons with frequency ω at a certain radial distance r to the beam axis and, hence, corresponds to the local spectrum of the beam. Note that $I(r, \omega)$ due to the cylindrical symmetry of X waves has no spatial dependencies other than r .

With the formulas above in mind, the reason for the X wave spectrum being local becomes clear. We can think of a twisted beam as the superposition of an infinite number of plane waves that interfere with each other. For a monochromatic beam this gives the well-known intensity pattern of concentric rings in the transversal plane. The position of these rings depends on the frequency of the beam. Because an X wave is constructed by convoluting monochromatic twisted beams over a spectral distribution, we measure a different intensity pattern for different frequencies. Vice versa, we find that the spectrum of an X wave depends on the point of observation.

Figure 1 shows the local spectrum of a $\omega_0 = 15$ eV X wave with three different pulse durations τ at three different r . As seen from the figure, the spectrum appears very sensitive to the axis distance r for a short pulse of $\tau = 150$ as (left panel). Here, the local spectrum is almost Gaussian for $r = 300$ nm, but multiple maxima appear if r is increased. A similar but not that distinct behavior is seen for slightly longer pulses ($\tau = 300$

as). For pulses with duration $\tau = 1$ fs, however, a variation of r results only in a different amplitude of a Gaussian-like-shaped $I(r, \omega)$. This behavior can be explained by the exponential prefactor in the integrand of Eq. (3) that approaches a delta function the longer the pulse becomes. In this limit ($\tau \rightarrow \infty$) the integration over ω in Eq. (3) is trivial and the spectrum of the (infinitely long) pulse is a delta peak at $\omega = 15$ eV independent of r .

Above we have derived the expression for the vector potential of a twisted pulse (3) and discussed its local spectrum. Before we can calculate the S matrix and cross section for the photoionization of atoms by such a pulse, we need to fix the geometry of the process. Consciously it is chosen to be very simple; as shown in Fig. 2, the longitudinal momentum \mathbf{k}_\parallel of the vortex beam and the momentum \mathbf{p} of the ejected electron are parallel. The target atom is located at \mathbf{b} in the transversal plane with respect to the beam axis. We will refer to its module $|\mathbf{b}| = b$ as the *impact parameter*.

In order to calculate the photoionization cross section, we need to evaluate the S matrix which is a measure for the probability amplitude of the process [40]. Under the assumption that the photon energies in the pulse are high enough to overcome the ionization threshold and the intensity of the pulse is low, it can be written, using first-order perturbation theory,

$$S = -i \int_{-\infty}^{\infty} dt e^{i(E_p - E_i)t} e^{-i\mathbf{k}_\perp \cdot \mathbf{b}} \times \langle \mathbf{p} m_s | \boldsymbol{\alpha} \cdot \mathbf{A}_{\theta_k m \lambda \omega_0}^{tw}(\mathbf{r}, t) | n_i j_i \mu_i \rangle, \quad (4)$$

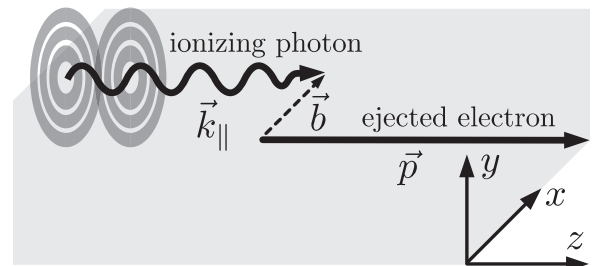


FIG. 2. Geometry of the photoionization by twisted light. The incident photons as well as the ejected electron propagate parallel to the z axis. Their separation is given by the vector \mathbf{b} .

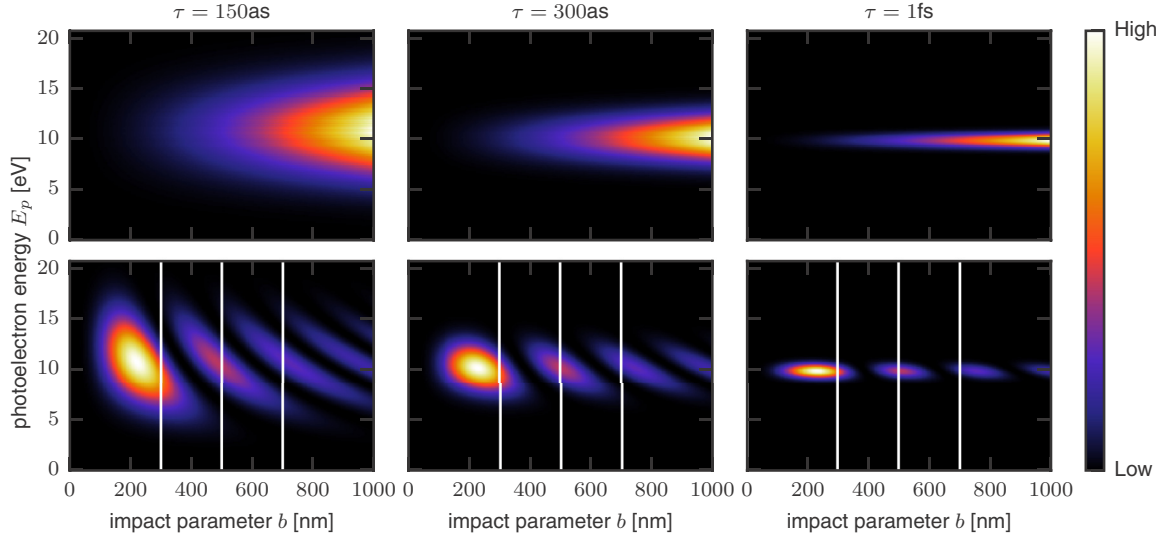


FIG. 3. Cross section $d\sigma_{\omega_0}/dp(p, b)$ (7) as a function of the impact parameter b and the photoelectron energy E_p . Calculations have been performed for the photoionization of neutral sodium by an X wave with $\omega_0 = 15$ eV for three different pulse durations: $\tau = 150$ as (left column), $\tau = 300$ as (center column), and $\tau = 1$ fs (right column), respectively. Results are shown for the opening angles $\theta_k = 0.1^\circ$ (top row) and $\theta_k = 10^\circ$ (bottom row). The projections of angular momenta are $\lambda = 1, m = 2$.

where α is the vector of Dirac matrices and the translation operator $\exp(-i\mathbf{k}_\perp \cdot \mathbf{b})$ specifies the location of the target in the beam [12,15,16]. Here, $\langle \mathbf{p} m_s |$ is a continuum solution of the Dirac equation with a well-defined asymptotic momentum \mathbf{p} , spin projection m_s , and energy E_p . The vector $|n_i j_i \mu_i\rangle$ describes a Dirac bound state with energy E_i , principal quantum number n_i , total angular momentum j_i , and angular momentum projection μ_i .

The time integration in Eq. (4) can be performed analytically and gives

$$S = -i \frac{\sqrt{2\pi}}{\Delta\omega} e^{-\frac{1}{2}(\frac{E_p - E_i - \omega_0}{\Delta\omega})^2} M_{fi}^{tw}(p, b). \quad (5)$$

Because of the particular choice of geometry, the matrix element

$$M_{fi}^{tw}(p, b) = \int \frac{d^2\mathbf{k}_\perp}{(2\pi)^2} a_{xm}(\mathbf{k}_\perp) e^{-i\mathbf{k}_\perp \cdot \mathbf{b}} \times \langle \mathbf{p} m_s | e^{i\mathbf{k} \cdot \mathbf{r}} \alpha \cdot \mathbf{u}_\lambda | n_i j_i \mu_i \rangle \quad (6)$$

depends only on the modules of the vectors \mathbf{p} and \mathbf{b} . The evaluation of $M_{fi}^{tw}(p, b)$ can be done using methods that have been outlined in our previous studies [12,16,41]. In order to describe the photoionization of neutral atoms, we here applied the single active electron approximation. In this approximation, the initial and final electron states are single-electron solutions of the Dirac equation with an effective potential [42]. In the present work all results are obtained for the ionization of the valence 3s electron of neutral sodium, where the effective potential is formed by the nucleus and the K- and L-shell electrons.

After we know how to evaluate the matrix element (6) we can calculate the energy differential cross section for the photoionization of an atom by a short twisted pulse. It is given

by the module squared of the S matrix (5),

$$\frac{d\sigma_{\omega_0}}{dp}(p, b) = \frac{2\pi}{\Delta\omega^2} e^{-\frac{(E_p - E_i - \omega_0)^2}{\Delta\omega^2}} \sum_{\mu_i m_s} \frac{1}{\sqrt{2j_i + 1}} |M_{fi}^{tw}(p, b)|^2, \quad (7)$$

where we assume that neither μ_i nor m_s is observed. It is noteworthy that the second line of Eq. (7) corresponds to the differential cross section for the photoionization of an atom by a continuous twisted wave with frequency $E_p - E_i$.

Using Eq. (7), we performed calculations for the ionization of a single sodium atom by a right circular polarized ($\lambda = 1$) X wave with center frequency $\omega_0 = 15$ eV and TAM projection $m = 2$. Figure 3 displays the cross section (7) for three different pulse lengths as a function of the impact parameter b and the energy of the ejected photoelectron E_p . By comparing the results column by column it can be seen that the scatter of photoelectron energies becomes narrower for larger values of τ . This can be understood from our discussion of Fig. 1, where we showed that the spectrum of the pulse approaches a delta function in the limit of a continuous wave ($\tau \rightarrow \infty$). Due to energy conservation, the energy distribution of photoelectrons exhibits the same behavior. The top row of Fig. 3 shows results for $\theta_k = 0.1^\circ$, which is close to the paraxial limit $\theta_k \rightarrow 0^\circ$. It can be seen that in this case only the amplitude but not the shape of the energy distribution depends on the impact parameter. In the case of a pure plane-wave pulse without any spatial structure, the width of the photoelectron energy distribution is the same as in the paraxial limit (cf. top right panel of Fig. 3) but the amplitude is constant for all impact parameters, because there are no intensity variations within the beam. However, if the ionizing pulse is far from both limits, $\tau \rightarrow \infty$ and $\theta_p \rightarrow 0$, it can be seen in Fig. 3 (bottom row, left and center panels) that both the shape and the width of the photoelectron spectrum strongly depend on the impact parameter. By comparing these results with Fig. 1, we find, again due to energy conservation,

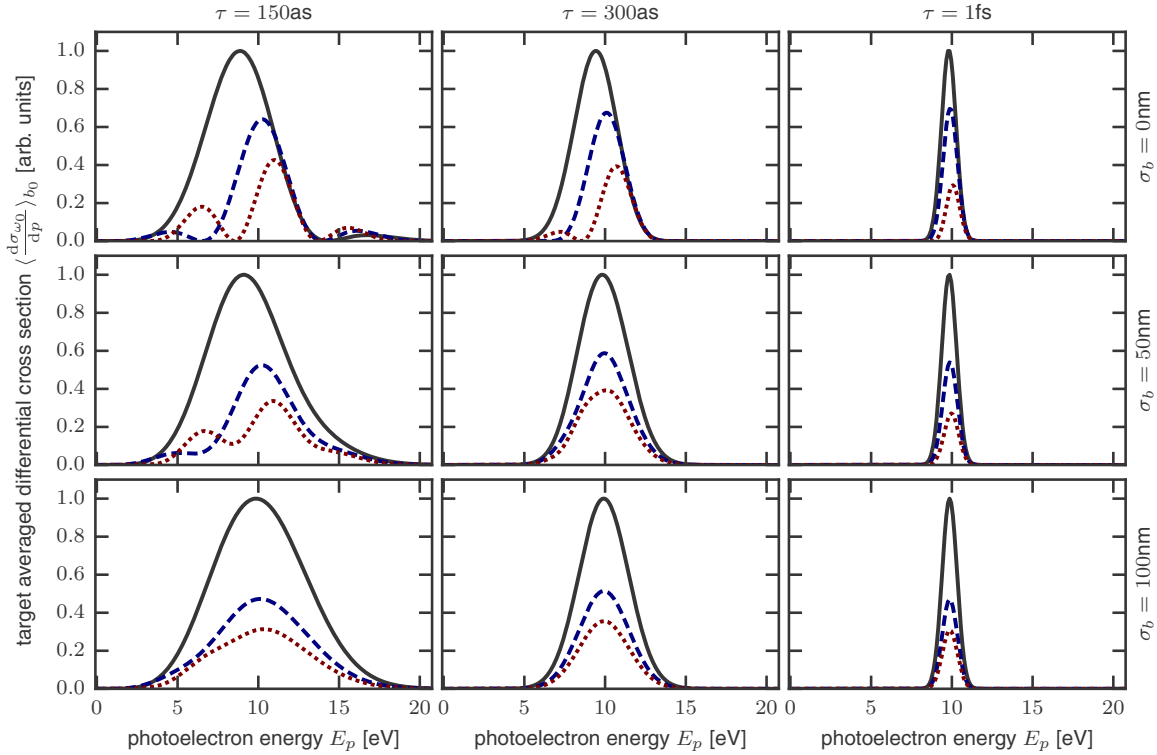


FIG. 4. Energy distribution of the photoelectrons for the photoionization of neutral sodium by an X wave with $m = 2$, $\lambda = 1$, and central frequency $\omega_0 = 15$ eV at three impact parameters: $b_0 = 300$ nm (black solid lines), $b_0 = 500$ nm (blue dashed lines), and $b_0 = 700$ nm (red dotted lines). Detailed calculations have been performed again for three pulse durations (left column: $\tau = 150$ as; center column: $\tau = 300$ as; right column: $\tau = 1$ fs) and three different target sizes (top row: $\sigma_b = 0$ nm; center row: $\sigma_b = 50$ nm; bottom row: $\sigma_b = 100$ nm). For better visibility all results have been normalized to one.

that the local spectrum of the ionizing X wave is reflected in the energy distribution of ejected electrons.

So far, we discussed the photoionization of a single atom placed at a particular impact parameter b with respect to the propagation axis of the X wave. Although such a localization of the target has been achieved lately [43], most photoionization experiments deal with extended (mesoscopic) targets. An extended target can be described by averaging the cross section (7) over a target distribution function $f_{\sigma_b}(\mathbf{b}_\perp)$ that characterizes the density of target atoms in the xy plane. This gives rise to the *target averaged* cross section,

$$\left\langle \frac{d\sigma_{\omega_0}}{dp}(p, b) \right\rangle_{b_0} = \int d\mathbf{b}_\perp f_{\sigma_b}(\mathbf{b}_\perp) \frac{d\sigma_{\omega_0}}{dp}, \quad (8)$$

where we assume a Gaussian target distribution with width σ_b around the point b_0 . For sufficiently small targets well away from the beam center, this target distribution can be approximated by

$$f_{\sigma_b}(\mathbf{b}_\perp) = \exp \left[-\frac{1}{2} \frac{(b - b_0)^2 + (b_0 \varphi_b)^2}{\sigma_b^2} \right]. \quad (9)$$

In contrast to the results for a single target atom, we expect that the dependence of the target averaged cross section (8) on the impact parameter will be washed out due to the integration over \mathbf{b}_\perp . Thus the local spectrum of the pulse will not be reflected in the photoelectron energy distribution as good as it is shown in Fig. 3. To analyze how exactly the target size σ_b affects

the visibility of the local spectrum in the energy distribution of photoelectrons, Fig. 4 compares the energy distribution of photoelectrons for three different σ_b . In the top row we display again results for the ionization of a single atom. These results correspond to cuts along the white vertical lines shown in Fig. 3 and reflect directly the local spectrum of the ionizing pulse. In the middle and bottom row of Fig. 4 results are shown for the same impact parameters but averaged over a $\sigma_b = 50$ nm and $\sigma_b = 100$ nm target, respectively. For the latter target size the results shown in each panel vary only in amplitude due to the different intensity of the ionizing pulse at different impact parameters. The overall shape of the photoelectron energy distribution, however, remains unaltered, a behavior that is changed as the target width becomes $\sigma_b \leq 50$ nm. As seen from Fig. 4, such a target is suitable to measure the local spectrum of a $\tau = 150$ as X wave. Yet, the spectrum of the longer $\tau = 300$ as pulse is only visible in the photoelectron energy distribution from a single target atom. The results for the longest considered X wave ($\tau = 1$ fs) exhibit no qualitative variation with the impact parameter. This is expected since we have shown in Fig. 1 that such a pulse has a spectrum that is Gaussian-like, independent on the position in the wave front.

In summary, we have investigated the ionization of neutral alkali-metal atoms by twisted attosecond pulses, also referred to as X waves. Our study is focused on the energy distribution of forward-emitted electrons. This energy distribution is determined by the spectrum of the ionizing pulse which, in turn, strongly depends on the pulse duration τ . As shown in the

present work, this remains true even for non-point-like targets. Therefore, we propose that the photoionization of alkali-metal atoms may be used as a probe process to study the (local) energy properties of X waves. Based on our calculations, it is shown that such a “mapping” of photon to electron energies is possible using atomic targets with size $\sigma_b \leq 50$ nm and pulse length $\tau \leq 300$ as. Recent experimental advances with Paul traps [43] and high harmonic optical vortices [25] indicate that these measurements might be possible in the near future. In addition, if not only the local spectrum but also the spin of the photoemitted electron is measured, our method can be used to locally characterize (twisted) pulses with

complex polarization patterns, e.g., cylindrically polarized X waves [39]. Such kinds of pulses have been recently discussed in the context of classical entanglement [44,45]. Moreover, our method might open up opportunities for transferring the classical entanglement from light fields to electron beams and even produce classically entangled electron vortex beams.

We thank Nils Becker for valuable discussions. R.A.M. acknowledges support from the RS-APS. The work reported in this Rapid Communication has been partially funded also by the QUTIF priority program of the DFG.

- [1] L. Allen, M. W. Beijersbergen, R. J. C. Spreeuw, and J. P. Woerdman, *Phys. Rev. A* **45**, 8185 (1992).
- [2] M. W. Beijersbergen, L. Allen, H. E. L. O. van der Veen, and J. P. Woerdman, *Opt. Commun.* **96**, 123 (1993).
- [3] G. Molina-Terriza, J. P. Torres, and L. Torner, *Nat. Phys.* **3**, 305 (2007).
- [4] S. Franke-Arnold, L. Allen, and M. Padgett, *Laser Photonics Rev.* **2**, 299 (2008).
- [5] *The Angular Momentum of Light*, edited by D. L. Andrews and M. Babiker (Cambridge University Press, Cambridge, U.K., 2013).
- [6] S. J. Van Enk and G. Nienhuis, *Europhys. Lett.* **25**, 497 (1994).
- [7] S. M. Barnett and L. Allen, *Opt. Commun.* **110**, 670 (1994).
- [8] L. Allen, M. Padgett, and M. Babiker, *Progress in Optics* (Elsevier, Amsterdam, 1999), Vol. 39, pp. 291–372.
- [9] I. Bialynicki-Birula and Z. Bialynicka-Birula, *J. Opt.* **13**, 064014 (2011).
- [10] A. M. Yao and M. J. Padgett, *Adv. Opt. Photonics* **3**, 161 (2011).
- [11] A. Bekshaev, K. Y. Bliokh, and M. Soskin, *J. Opt.* **13**, 053001 (2011).
- [12] A. Surzhykov, D. Seipt, and S. Fritzsche, *Phys. Rev. A* **94**, 033420 (2016).
- [13] H. He, M. E. J. Friese, N. R. Heckenberg, and H. Rubinsztein-Dunlop, *Phys. Rev. Lett.* **75**, 826 (1995).
- [14] M. F. Andersen, C. Ryu, P. Cladé, V. Natarajan, A. Vaziri, K. Helmerson, and W. D. Phillips, *Phys. Rev. Lett.* **97**, 170406 (2006).
- [15] O. Matula, A. G. Hayrapetyan, V. G. Serbo, A. Surzhykov, and S. Fritzsche, *J. Phys. B* **46**, 205002 (2013).
- [16] H. M. Scholz-Marggraf, S. Fritzsche, V. G. Serbo, A. Afanasev, and A. Surzhykov, *Phys. Rev. A* **90**, 013425 (2014).
- [17] I. A. Litvin, A. Dudley, and A. Forbes, *Opt. Express* **19**, 16760 (2011).
- [18] K. Bezuhanov, A. Dreischuh, G. G. Paulus, M. G. Schätzel, and H. Walther, *Opt. Lett.* **29**, 1942 (2004).
- [19] I. G. Marienko, J. Strohaber, and C. Uiterwaal, *Opt. Express* **13**, 7599 (2005).
- [20] H. I. Sztul, V. Kartazayev, and R. R. Alfano, *Opt. Lett.* **31**, 2725 (2006).
- [21] F. Eilenberger, K. Prater, S. Minardi, R. Geiss, U. Röpke, J. Kobelke, K. Schuster, H. Bartelt, S. Nolte, A. Tünnermann, and T. Pertsch, *Phys. Rev. X* **3**, 041031 (2013).
- [22] G. Pariente and F. Quéré, *Opt. Lett.* **40**, 2037 (2015).
- [23] M. Zürich, C. Kern, P. Hansinger, A. Dreischuh, and C. Spielmann, *Nat. Phys.* **8**, 743 (2012).
- [24] C. Hernández-García, A. Picón, J. San Román, and L. Plaja, *Phys. Rev. Lett.* **111**, 083602 (2013).
- [25] G. Gariépy, J. Leach, K. T. Kim, T. J. Hammond, E. Frumker, R. W. Boyd, and P. B. Corkum, *Phys. Rev. Lett.* **113**, 153901 (2014).
- [26] E. Hemsing, A. Knyazik, M. Dunning, D. Xiang, A. Marinelli, C. Hast, and J. B. Rosenzweig, *Nat. Phys.* **9**, 549 (2013).
- [27] J. Bahrdrdt, K. Holldack, P. Kuske, R. Müller, M. Scheer, and P. Schmid, *Phys. Rev. Lett.* **111**, 034801 (2013).
- [28] P. R. Ribič, D. Gauthier, and G. De Ninno, *Phys. Rev. Lett.* **112**, 203602 (2014).
- [29] P. Saari and H. Sonajalg, *Laser Phys.* **7**, 32 (1997).
- [30] *Localized Waves*, edited by H. E. Hernández-Figueroa (Wiley, Hoboken, NJ, 2008).
- [31] G. Valiulis, J. Kilius, O. Jedrkiewicz, A. Bramati, S. Minardi, C. Conti, S. Trillo, A. Piskarskas, and P. D. Trapani, *Quantum Electronics and Laser Science Conference* (Optical Society of America, Washington, D.C., 2001), p. QPD10.
- [32] C. Conti, S. Trillo, P. Di Trapani, G. Valiulis, A. Piskarskas, O. Jedrkiewicz, and J. Trull, *Phys. Rev. Lett.* **90**, 170406 (2003).
- [33] A. Ciattoni and C. Conti, *J. Opt. Soc. Am. B* **24**, 2195 (2007).
- [34] C. Conti and S. Trillo, *Phys. Rev. Lett.* **92**, 120404 (2004).
- [35] Y. Lahini, E. Frumker, Y. Silberberg, S. Droulias, K. Hizanidis, R. Morandotti, and D. N. Christodoulides, *Phys. Rev. Lett.* **98**, 023901 (2007).
- [36] M. Heinrich, A. Szameit, F. Dreisow, R. Keil, S. Minardi, T. Pertsch, S. Nolte, A. Tünnermann, and F. Lederer, *Phys. Rev. Lett.* **103**, 113903 (2009).
- [37] M. Ornigotti, C. Conti, and A. Szameit, *Phys. Rev. Lett.* **115**, 100401 (2015).
- [38] M. Ornigotti, C. Conti, and A. Szameit, *Phys. Rev. A* **92**, 043801 (2015).
- [39] M. Ornigotti, C. Conti, and A. Szameit, *J. Opt.* **18**, 075605 (2016).
- [40] L. Landau, E. Lifshitz, V. Berestetskii, L. Pitaevskii, and J. Sykes, *Relativistic Quantum Theory Part I*, Course of Theoretical Physics No. 4 (Pergamon, New York, 1971).
- [41] T. Radtke, S. Fritzsche, and A. Surzhykov, *Phys. Rev. A* **74**, 032709 (2006).
- [42] S. Fritzsche, *Comput. Phys. Commun.* **183**, 1525 (2012).
- [43] C. T. Schmiegelow, J. Schulz, H. Kaufmann, T. Ruster, U. G. Poschinger, and F. Schmidt-Kaler, *Nat. Commun.* **7**, 12998 (2016).
- [44] P. Ghose and A. Mukherjee, *Rev. Theor. Sci.* **2**, 274 (2014).
- [45] A. Aiello, F. Töppel, C. Marquardt, E. Giacobino, and G. Leuchs, *New J. Phys.* **17**, 043024 (2015).